Thin Solid Films 517 (2009) 3717–3720

Contents lists available at ScienceDirect

Thin Solid Films

journal homepage: www.elsevier.com/locate/tsf

# Surface textured molybdenum zinc oxide for light diffusion enhancement

Ching-Ming Hsu *, Hon-Bin Lin, Wen-Tuan Wu

*Department of Electro-Optical Engineering, Southern Taiwan University, 1 Nan-Tai Street, Yung-Kang City, Tainan County, Taiwan 710, Republic of China*

ARTICLE INFO

*Article history:*
Received 14 February 2008
Received in revised form 13 December 2008
Accepted 15 December 2008
Available online 25 December 2008

*Keywords:*
Molybdenum
Zinc oxide
Surface texture
Light trapping

ABSTRACT

Surface textures have been fabricated on a molybdenum doped zinc oxide (MZO) film using a shadow mask in a co-sputter process. The surface textures yielded 5.3% and 10.1% of light diffusion in the visible light region for MZO films with a thickness of 100 nm and 200 nm, respectively. Light diffusion in the near infra-red region was slightly less with 4.5% for the 100 nm MZO film and 8.9% for the 200 nm MZO film. The enhanced light diffusion will be beneficial to the light trapping efficiency of a-Si/μ-Si based thin film solar cells.



## 1. Introduction

Transparent conductive oxides (TCO) with textured surfaces have been commonly used as electrodes in thin film solar cells [1–4]. The textured surface allows the incoming solar light to diffuse laterally into the thin film absorbers of a solar cell. Since the traveling length of the diffused light in the absorber layers is a number of magnitudes of order longer than that of the directly transmitting light, the light trapping efficiency would be largely enhanced and thus lead to the improved power efficiency. For amorphous (a-Si)/microcrystalline (μ-Si) based thin film solar cells, lateral light diffusion is particularly important because of the thin thickness required in a-Si (due to the light-induced degradation) and the low absorption efficiency in μ-Si [1]. Yielding textured surfaces is then crucial when employing TCO films to serve as a transparent conductive electrode in the a-Si/μ-Si solar cells in addition to the basic requirements of high optical transparency and low electrical resistance.

Zinc oxide (ZnO) has been a highly noticed TCO material for the applications in thin film solar cells for its low cost, high optical transparency in the near infra-red region and good chemical stability during a-Si depositions [5–8]. Forming textured surfaces is inclusively one of the important issues when fabricating ZnO films. Several approaches have been proposed to obtain surface textures on ZnO films, including the direct growth by well-controlled chemical vapor deposition [9,10] and the post chemical etching [11,12]. Synthesis of optical grating patterns on film surfaces by photolithography technique has also been demonstrated to be able to perform surface diffusion effect [13,14]. These methods however employ processes of high cost such as photolithography patterning, or encounter the problem of limited physical structure of surface textures when using direct growth or chemical etching.

In this article we proposed a method that could fabricate molybdenum (Mo) doped ZnO (MZO) films with surface textures of a desired geometry without additional post-treatments. This method employs a shadow mask attached to a substrate, which allows surface textures to form through the opening of the mask during film deposition. Since the physical dimension and the shape of the opening are defined directly on the shadow mask, surface textures with a well-controlled geometry are obtainable. The optical diffusion effect caused by the textured surface of ZnO films was investigated. The effect of MZO thickness and MZO film/texture interface to the optical diffusion was also discussed.

## 2. Experimental details

A molybdenum doped ZnO film with a thickness of 100 nm or 200 nm was first deposited on a 50 mm × 50 mm glass substrate at 300 °C using a magnetron co-sputter approach as illustrated in Fig. 1. Mo was sputtered with a dc power of 10 W whereas ZnO with an rf power of 150 W. The substrate was placed 10 cm above the sputter sources and was rotated at a speed of 15 rpm. The concentration of Mo was controlled by the opening area of a slit shutter located in front of the Mo sputter source. On the MZO film, round surface textures were formed by the deposition of MZO through a metallic shadow mask that was attached to the substrate. The samples were then annealed in vacuum at 350 °C for 1 h to enhance the electrical and optical properties of the MZO films.

MZO films with four types of geometrical structures were fabricated, (a) 100 nm, (b) 100 nm with surface textures, (c) 200 nm and (d) 200 nm with surface textures. These films were characterized by energy dispersive X-ray analysis using Hitachi S4100-EDS for Mo

* Corresponding author. Tel.: +886 6 2533131x3360; fax: +886 6 2432912.
*E-mail address:* tedhsu@mail.stut.edu.tw (C.-M. Hsu).

0040-6090/$ – see front matter © 2008 Elsevier B.V. All rights reserved.
doi:10.1016/j.tsf.2008.12.038

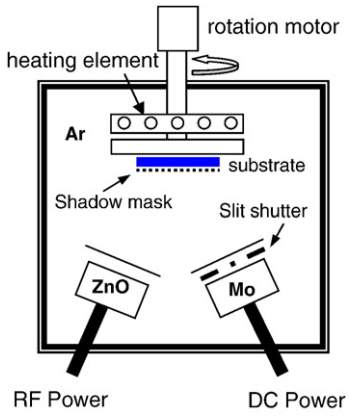


**Fig. 1.** Schematic of a co-sputter apparatus for fabricating surface textured MZO film.

concentration at acceleration voltage of 15 kV and collection time of 60 s Thickness was measured using surface profilometry (ET-4000 α-step). Optical transmittance was measured using Hitachi UV 3310 and the 4-point probe method was used for obtaining the sheet resistivity (4 Dimensions 280SI).

## 3. Results and discussions

### 3.1. Electrical and optical properties of MZO films

The lowest sheet resistivity of the MZO film in this study was $3.2\times10^{-3}$ Ω cm$^2$, which was obtained from the film with 1.85 wt.% concentration of Mo and after thermal annealing. Since the goal of this work was to investigate the optical diffusion by MZO surface textures, the electrical performance of the MZO film was not further improved. Surface textures were then only processed on top of the MZO film with this optimal sheet resistivity. The following discussions will mainly focus on the optical effects caused by the MZO surface textures.

Fig. 2 shows the optical spectra of MZO films in the wavelength region from 350 nm to 1100 nm. The measurement was conducted with light incident from the glass side at normal angle to the sample. It can be seen that in the entire wavelength region MZO films with surface textures (type (b) and (d)) performed lower optical transmittance than the plain MZO films (type (a) and (c)). Clearly the causes of the drop in the optical transmittance are related with the MZO textures fabricated on the MZO films. We examined the morphology of these textures and analyzed the possible causes how they influence the optical behavior of the incident light.

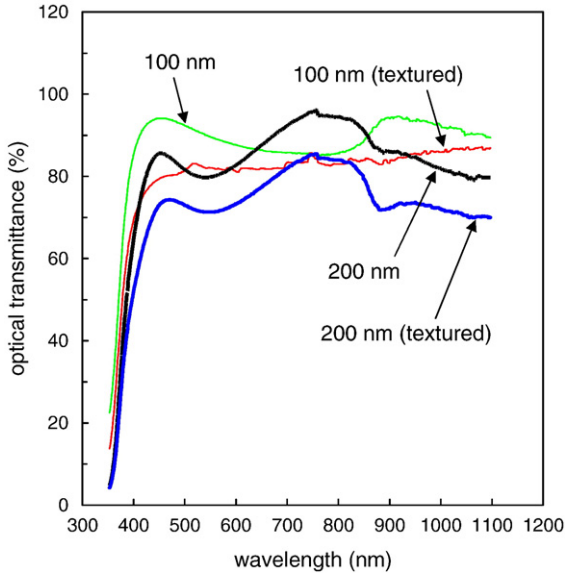


**Fig. 2.** Optical spectra of MZO films with various physical structures in the wavelength region from 350 to 1100 nm.

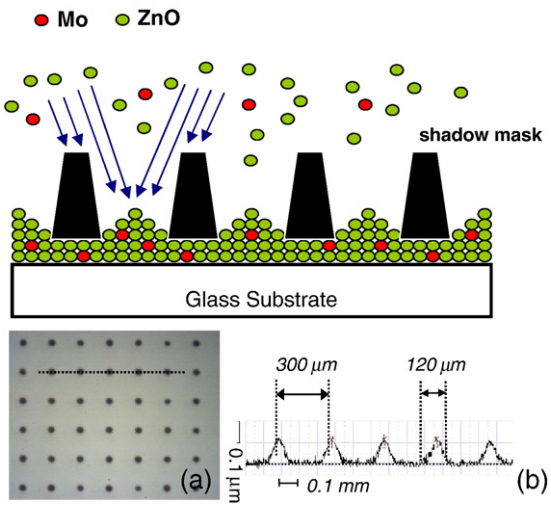


**Fig. 3.** (a) optical microscope image; (b) a-step profile of the surface textured MZO film. Above shows the shadowing effect of the shadow mask.

### 3.2. Physical dimensions of MZO films

Fig. 3(a) and (b) show the optical microscope image and α-step profile of the surface textured MZO film, respectively. The dark spots in Fig. 3(a) represent where the MZO textures locate. These textures are nearly identical and spread evenly on the MZO film, suggesting a well controlled and periodic texture pattern can be formed with the shadow mask approach. Above the figures schematically illustrates how these textures are formed by the shadowing effect of the metallic shadow mask. Observed from the a-step profiling in Fig. 3(b), these textures appear in spherical shape and are 300 μm pitched to each other. The MZO texture was measured to have physical dimensions of

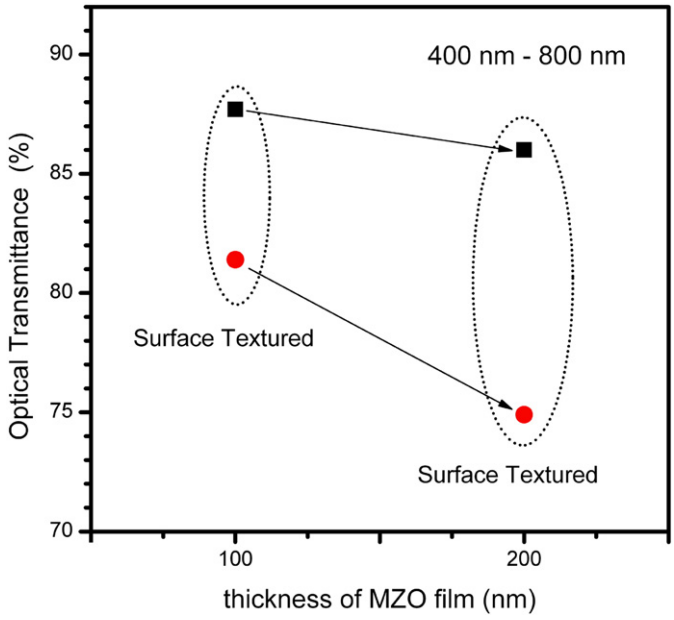


**Fig. 4.** Averaged optical transmittance of MZO films with various physical structures in the visible light region from 400 to 800 nm.

110 nm in height and 120 um in diameter that is close to the size of the opening of shadow mask. From the physical dimensions, these textures were calculated to cover around 12.6% of the total area of the MZO film.

### 3.3. Optical effects of MZO films with surface textures

Fig. 4 shows the averaged optical transmittance of the MZO films with various structures in the visible light region (from 400 to 800 nm). It can be seen that the optical transmittance drops from 87.7% to 86.0% when the thickness of MZO increases from 100 nm to 200 nm, whereas it drops to 81.4% with a textured surface. This suggested that the surface textures on the 100 nm MZO film reduced 6.1% of the incident light entering the photo-detector of the spectrometer, provided the thickness effect of the surface textures on the optical transmittance is the maximal value of 0.2% (the texture occupied area 12.6% × the optical drop from 87.7% to 86.0%). These escaping photons are likely attribute to the optical deflection when traveling through the textured surfaces of the MZO film and then not detected by the photo-detector. We also processed a MZO film with a 100 nm/100 nm double layer to investigate the influence from the MZO film/texture interfaces. The optical transmittance of this stacked MZO film is only 0.8% lower than that of the continuously coated MZO film of 200 nm. Hence the light trapping at the MZO/MZO interface should not be the main cause for the drop in optical transmittance of the surface textured MZO films. We estimated that at least 5.3% of light was laterally diffused by the surface textures. The dark spots in the optical microscope image (Fig. 3(a)) also give evidence that light diffused on the surface textures.

For the 200 nm MZO film with surface textures, a more severe drop in the optical transmittance (74.9%) was observed. Again if the optical absorption from the textures (0.2%) and the light trapping at film/texture (0.8%) are taken into account, the surface textures actually diffuse around 10.1% of the incoming light. This means that the surface textures could result in much higher light diffusion efficiency when the thickness of initial MZO film is increased. The schematic light path in the MZO structures, as illustrated in Fig. 5, can explain this phenomenon. In case (a), light travels through the glass and 100 nm MZO film with a certain degree of reflection and scattering at the air/glass/MZO/air interfaces (only that at glass/MZO is plotted). Light being detected by the photo-detector counts for those not absorbed in the sample and not deflected or reflected. In case (b), a portion of incident light deflects at the texture surface and is not detected by the photo-detector, resulting in a reduction in optical transmittance. Scattered light at glass/MZO interface may also deflect at the texture surface, which contributes another part of the optical drop. Case (c) has the same situation as in the case (a) except a longer traveling path of photons in the MZO film that causes more optical absorption. In case (d), deflection angles of the scattered light (from the glass/MZO interface) at the texture surface become larger so that more light scatter away from the photo-detector. This further decreases the optical transmittance, in other words, increases light diffusion. The diffused light when travel into a-Si or μ-Si films could largely enhance the light trapping efficiency because it can travel in the Si absorbers at a distance of thousands of microns rather than the thickness of the absorbers (<a few microns) as being discussed by Zeng [15].

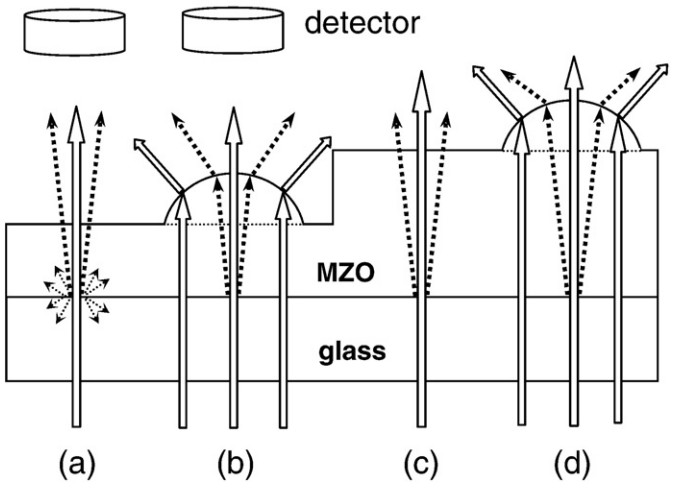


**Fig. 5.** Schematics of the light path for (a) 100 nm MZO film, (b) 100 nm MZO film with surface textures, (c) 200 nm MZO film and (d) 200 nm MZO film with surface textures. The dotted lines represent the scattered light at the glass/MZO interfaces.

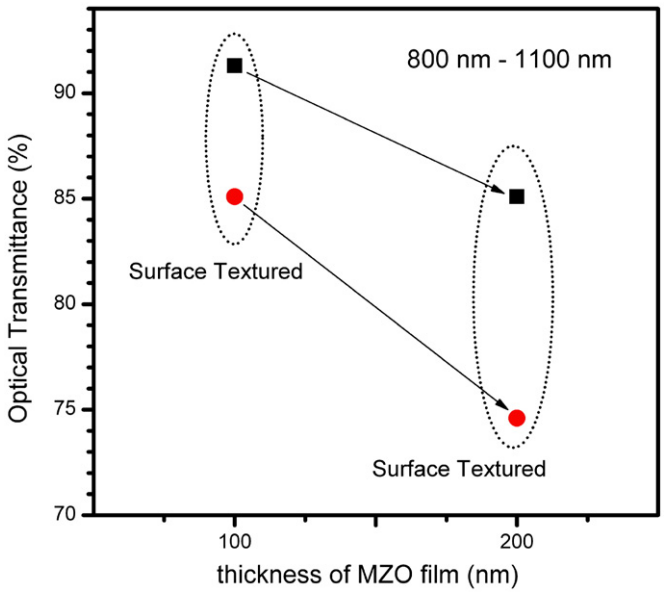


**Fig. 6.** Averaged optical transmittance of MZO films with various physical structures in the infra-red region from 800 to 1100 nm.

Fig. 6 shows the averaged optical transmittance of MZO films in the near infra-red region (from 800 to 1100 nm). The optical transmittance is 91.2% and 85.1% for the 100 nm MZO film and the film with surface textures, respectively. For the 200 nm MZO film, the optical transmittance is 85.1% and it drops to 74.6% for the film with surface textures. Considering the absorption from the textures (~0.8% in this case) and the light trapping at MZO/texture (~0.8%) as discussed earlier, surface textures diffuse 4.5% and 8.9% of the incident light for the 100 nm and 200 nm MZO film, respectively. This observation indicates that the light diffusion efficiency caused by the surface textures is slightly less in the NIR region. However the light trapping efficiency in both a-Si (high absorption in visible light region) and μ-Si (high absorption in NIR region) absorbers is expected to be improved with this surface textured MZO approach.

## 4. Conclusions

This work has demonstrated that surface textures with a desired geometry could be fabricated on MZO films by sputter deposition through a micro shadow mask. The surface textures effectively deflected the incident light on the film surface, and yielded 5.3% and 10.1% of light diffusion in the visible light region for MZO films with a thickness of 100 nm and 200 nm, respectively. Light diffusion in the near infra-red region appeared to be slightly less with an optical transmittance drop of 4.5% for the 100 nm film and 8.9% for the 200 nm film. The diffused light is expected to enhance the light trapping efficiency of a-Si/μ-Si based thin film solar cells.

## Acknowledgement

The authors would like to thank the National Science Council of the Republic of China, Taiwan, for financially supporting this work under Contract No. NSC-96-2221-E-218-019-MY3.

## References

[1] J. Muller, B. Rech, J. Springer, Milan Vanecek, Sol. Energy 77 (2004) 917.
[2] H. Iida, T. Mishuku, I. Sakata, Y. Hayashi, IEEE Electron Device Lett. 5 (3) (1984) 65.
[3] E. Fortunato, D. Ginley, H. Hasono, D. Paine, MRS Bull. 32 (2) (2007) 46.
[4] S. Hagedus, W. Buchanan, X. Liu, R. Gordon, IEEE Proceedings of the 25th Photovoltaic Solar Cells, Washington, U.S.A., May 13–17, 1996, p. 1129.
[5] T. Minami, MRS Bull. 25 (8) (2000) 38.
[6] J.B. Webb, D.F. Williams, Appl. Phys. Lett. 39 (8) (1981) 640.
[7] L.R. Weiberg, C.F. Grain, R.R. Addiss, Appl. Phys. Lett. 27 (8) (1975) 440.
[8] A. Shah, J. Meier, A. Buechel, U. Kroll, J. Steinhauser, F. Meillaud, H. Schade, D. Domine, Thin Solid Films 502 (2006) 292.
[9] S. Fay, L. Feitknecht, R. Schluchter, U. Kroll, E. Vallat-Sauvain, A. Shah, Sol. Energy Mater. Sol. Cells 90 (2006) 2960.
[10] R. Groenen, J. Loffler, J. Linden, R. Schropp, M. van der Sanden, Thin Solid Films 492 (2005) 298.
[11] V. Sttinger, F. Ruske, W. Werner, B. Szyszka, B. Rech, J. Hupkes, G. Schope, Steibig, Thin Solid Films 496 (2006) 16.
[12] J. Hupkes, B. Rech, O. Kluth, T. Repmann, B. Zwaygardt, J. Muller, R. Drese, M. Wuttig, Sol. Energy Mater. Sol. Cells 90 (2006) 3054.
[13] H. Stiebig, N. Senoussaoui, T. Brammer, J. Muller, Sol. Energy Mater. Sol. Cells 90 (2006) 3031.
[14] C. Eisele, C.E. Nebel, M. Stutzmann, J. Appl. Phys. 89 (12) (2001) 7722.
[15] L. Zeng, Y. Yi, C. Hong, J. Liu, N. Feng, X. Duan, L.C. Kimerling, B.A. Almariu, Appl. Phys. Lett. 89 (2006) 111.